Identifying Dehn functions of Bestvina–Brady groups from their defining graphs

Yu-Chan Chang[1]

Abstract
Let Γ be a finite simplicial graph such that the flag complex on Γ is a 2-dimensional triangulated disk. We show that with some assumptions, the Dehn function of the associated Bestvina–Brady group is either quadratic, cubic, or quartic. Furthermore, we can identify the Dehn function from the defining graph Γ.

Keywords Bestvina–Brady groups · Dehn functions · Right-angled Artin groups

Mathematics Subject Classification (2020) 20F65 · 20F05 · 20E06 · 20E05

1 introduction

Dehn functions are one of the quasi-isometry invariants of finitely presented groups, and they have been studied by many people. One of the reasons people study Dehn functions is that they are related to the solvability of the word problem for finitely presented groups. That is, a finitely presented group has a solvable word problem if and only if its Dehn function is recursive. Besides the solvability of the word problem, Dehn functions can also detect certain structures in groups. For example, a group is hyperbolic if and only if it has a linear Dehn function [14]. We refer to [8] for background on Dehn functions. In this paper, we study Dehn functions of Bestvina–Brady groups, which are a class of subgroups of right-angled Artin groups.

Given a finite simplicial graph Γ, the associated right-angled Artin group A_Γ is generated by the vertices of Γ. The relators are commutators: two generators u, v commute if and only if they are adjacent vertices of Γ. Right-angled Artin groups have become an important objects that people study in geometric group theory; see [11] for a general survey. They are known to be CAT(0) groups; both categories of groups have at most quadratic Dehn functions. But subgroups can have larger Dehn functions. Brady and Forester [4] gave examples of CAT(0) groups that contain finitely presented subgroups whose Dehn functions are of the form n^ρ,

---

✉ Yu-Chan Chang
yuchanchang74321@gmail.com ; yu-chan.chang@emory.edu

1 Oxford College of Emory University, 801 Emory Street, Oxford, GA 30054, USA
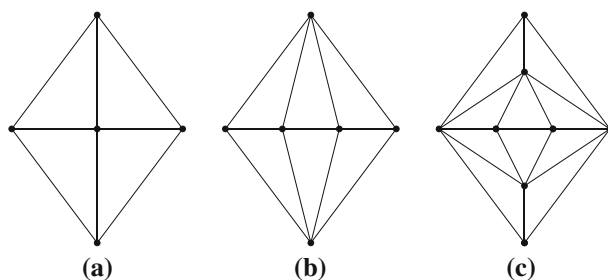
Fig. 1 Triangulated disks whose interior dimensions are 0, 1, and 2, respectively

for a dense set of $\rho \in [2, \infty)$. Brady and Soroko [6] proved that for each positive integer ρ, there is a right-angled Artin group that contains a finitely presented subgroup whose Dehn function is n^ρ.

For a right-angled Artin group A_Γ, the associated Bestvina–Brady group H_Γ is defined to be the kernel of the homomorphism $A_\Gamma \to \mathbb{Z}$, which sends all the generators of A_Γ to 1. This kernel had been studied prior to Bestvina–Brady. Stallings [16] constructed a group that is finitely generated but not finitely presented. This group can be realized as the Bestvina–Brady group $H_\Gamma = \ker(F_2 \times F_2 \to \mathbb{Z})$, where Γ is a cycle graph C_4. When Γ is taken to be the $(n + 1)$-fold join of two vertices, the right-angled Artin group on Γ is the n-copies of F_2, and Bieri [3] proved that the associated Bestvina–Brady group $H_\Gamma = \ker(F_2 \times \cdots \times F_2 \to \mathbb{Z})$ satisfies the finiteness property $\mathbf{FP}_n$ but not $\mathbf{FP}_{n+1}$. Bestvina and Brady [2] gave a systematic construction of groups that satisfy some finiteness properties but not others. Moreover, there are Bestvina–Brady groups that are either counterexamples to the Eilenberg–Ganea Conjecture or counterexamples to the Whitehead Conjecture ([2], Theorem 8.7).

Dison proved that the Dehn functions of Bestvina–Brady groups are bounded above by quartic polynomials [13]. We are interested in knowing whether all the Bestvina–Brady groups have Dehn functions of the form n^α, $\alpha = 1, 2, 3$ or 4. Our motivation is Brady's examples in ([5], Part I), where he gave Bestvina–Brady groups that realize quadratic, cubic, and quartic Dehn functions. In each of those examples, the flag complex on the defining graph Γ, denoted by Δ_Γ, is a 2-dimensional triangulated disk with square boundary. In this paper, we prove that the Dehn functions of Bestvina–Brady groups H_Γ with such restrictions on the defining graphs Γ are of the form n^α, $\alpha = 1, 2, 3$ or 4. Furthermore, we provide a way to identify the Dehn functions of those Bestvina–Brady groups by their defining graphs. A simplex of a 2-dimensional triangulated disk D is called an *interior simplex* if none of its faces are on ∂D. If D has interior d-simplices, and no other interior k-simplices, $k > d$, then we say that D has the *interior dimension* d, denoted by $\dim_I(D) = d$. If D has no interior simplices, then we define $\dim_I(D) = 0$. Our main result is the following theorem:

Theorem 1.1 *Let Γ be a finite simplicial graph such that Δ_Γ is a 2-dimensional triangulated disk whose boundary is a square. If $\dim_I(\Delta_\Gamma) = d$ for $d \in \{0, 1, 2\}$, then $\delta_{H_\Gamma}(n) \cong n^{d+2}$.*
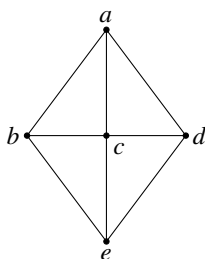
Example 1.2 The flag complexes on the graphs shown in Fig. 1 are 2-dimensional triangulated disks with square boundary, and they have interior dimensions 0, 1, and 2, respectively.

We now briefly discuss the proof of Theorem 1.1. When $\dim_I(\Delta_\Gamma) = 0$, we can eliminate the square boundary condition on Δ_Γ; see Theorem 3.1. In this case, the Bestvina–Brady group H_Γ has a graph of groups decomposition, where the edge groups are infinite cyclic,

and the vertex groups are right-angled Artin groups. In fact, these Bestvina–Brady groups are CAT(0), therefore, their Dehn functions are at most quadratic. Since we assume that the flag complexes are triangulated disks, the associated Bestvina–Brady groups have $\mathbb{Z}^2$ subgroups. Thus, these Bestvina–Brady groups are not hyperbolic and have at least quadratic Dehn functions. We remark that some cases of $\dim_I(\Delta_\Gamma) = 0$ in Theorem 1.1 can be obtained by a result of Carter and Forester [10]:

Theorem 1.3 ([10], Corollary 4.3) *If a finite simplicial graph Γ is a join of three graphs $\Gamma = \Gamma_1 * \Gamma_2 * \Gamma_3$, then δ_{H_Γ} is quadratic.*

Example 1.4 Let Γ be the graph in Fig. 1a. Label the vertices as follows:

Let $\Gamma_1 = \{c\}$, $\Gamma_2 = \{b, d\}$, and $\Gamma_3 = \{a, e\}$, then $\Gamma = \Gamma_1 * \Gamma_2 * \Gamma_3$. Therefore, δ_{H_Γ} is quadratic by Theorem 1.3. It also follows from Theorem 1.1 that δ_{H_Γ} is quadratic.

In [5], Brady proved that the Bestvina–Brady group on the graph shown in Fig. 1b has a cubic Dehn function. This graph can be seen as the suspension of a path of length 3. When $\dim_I(\Delta_\Gamma) = 1$, we prove that Γ is the suspension of a path, and we show that the associated Bestvina–Brady group has a cubic Dehn function. To achieve the cubic upper bound, we use the *corridor schemes* [4] to analyse the van Kampen diagrams carefully. Lemma 4.10 is the main technical result of this paper. In this technical lemma, we prove that the area of a special region, called a *stack*, in a van Kampen diagram is bounded above by a cubic function of the perimeter of that region. This result allows us to obtain the desired cubic upper bound; see Lemma 4.15 for a detail proof.

Since there is a universal quartic upper bound on the Dehn functions of Bestvina–Brady groups, the remaining cases are the cubic and quartic lower bounds for $\dim_I(\Delta_\Gamma) = 1, 2$, respectively. In [1], the authors introduced the *height-pushing map* to obtain the lower bound on the higher Dehn functions of orthoplex groups. Their method can be adapted to our proof to obtain the desired lower bounds. We want to point out that their theorem ([1], Theorem 5.1) recovers Dison's quartic upper bound in [13]. We have discussed all the cases of our main result Theorem 1.1.

Denote K_4 to be the complete graph on four vertices. Note that the assumption of the flag complex Δ_Γ being 2-dimensional is equivalent to saying that the graph Γ does not have K_4 subgraphs. Suppose a given graph Γ whose flag complex is a triangulated disk but not necessarily 2-dimensional or has square boundary. If Γ contains a subgraph that satisfies the assumptions of Theorem 1.1, then we can obtain a lower bound on the Dehn function of the associated Bestvina–Brady group H_Γ:

Proposition 1.5 *Let Γ be a finite simplicial graph such that Δ_Γ is simply-connected. If Γ contains an induced subgraph Γ' such that $\Delta_{\Gamma'}$ is a 2-dimensional triangulated subdisk of Δ_Γ that has square boundary and $\dim_I(\Delta_{\Gamma'}) = d$ for $d \in \{0, 1, 2\}$, then $n^{d+2} \preceq \delta_{H_\Gamma}(n)$.*

This paper is organized as follows. Section 2 provides some necessary background. In Sect. 3, we prove the case of $\dim_I(\Delta_\Gamma) = 0$ without the square boundary assumption. Section 4 is devoted to the proof of Theorem 1.1. In Sect. 5, we prove Proposition 1.5.

2 preliminaries

2.1 Dehn functions

Let G be a group with a finite presentation $\mathcal{P} = \langle S | \mathcal{R} \rangle$. Let w be a word in $F(S)$ that represents the identity of G, denoted by $w \equiv_G 1$. The *area* of w, denoted by $\mathrm{Area}(w)$, is defined as follows:

$$\mathrm{Area}(w) = \min \left\{ N \ \middle|\ w \overset{F(S)}{=} \prod_{i=1}^{N} x_i r_i^{\pm 1} x_i^{-1}, x_i \in F(S), r_i \in \mathcal{R} \right\},$$

where $F(S)$ is the free group generated by S. The *Dehn function* $\delta_G : \mathbb{N} \to \mathbb{N}$ of a group G over the presentation $\mathcal{P} = \langle S | \mathcal{R} \rangle$ is defined by

$$\delta_{\mathcal{P}}(n) = \max \left\{ \mathrm{Area}_G(w) \ \middle|\ w \equiv_G 1, |w| \le n \right\},$$

where $|w|$ denotes the length of the word w.

Definition 2.1 Let $f, g : [0, \infty) \to [0, \infty)$ be two functions. We say that f is *bounded above* by g, denoted by $f \preceq g$, if there is a number $C > 0$ such that $f(n) \le Cg(Cn + C) + Cn + C$ for all $n > 0$. We say that f and g are $\simeq$-*equivalent*, or simply *equivalent*, denoted by $f \simeq g$, if $f \preceq g$ and $g \preceq f$.

If $\mathcal{P}_1$ and $\mathcal{P}_2$ are finite presentations of a group G, then $\delta_{\mathcal{P}_1}$ is equivalent to $\delta_{\mathcal{P}_2}$; we refer to [8] for a proof of this fact. We denote the $\simeq$-equivalent class of G by δ_G, and call it the *Dehn function* of G. We say that the Dehn function δ_G is *linear*, *quadratic*, *cubic* or *quartic* if for all $n \in \mathbb{N}$, $\delta_G(n) \simeq n$, $\delta_G(n) \simeq n^2$, $\delta_G(n) \simeq n^3$ or $\delta_G(n) \simeq n^4$, respectively.

2.2 Right-angled Artin groups, Bestvina–Brady groups, and the Dicks–Leary presentation
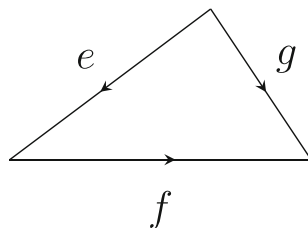
Let Γ be a finite simplicial graph and $\mathrm{V}(\Gamma)$ the set of vertices of Γ. The *right-angled Artin group* A_Γ associated to Γ has the following presentation:

$$A_\Gamma = \left\langle \mathrm{V}(\Gamma) \ \middle|\ [v_i, v_j] \text{ whenever } v_i \text{ and } v_j \text{ are connected by an edge of } \Gamma \right\rangle.$$

When Γ is a complete graph K_n on n vertices, $A_\Gamma = \mathbb{Z}^n$; when Γ is a set of n distinct points, $A_\Gamma = F_n$, the free group of rank n.

For each finite simplicial graph Γ, its associated right-angled Artin group A_Γ is the fundamental group of a cubical complex X_Γ, called the *Salvetti complex*. It is well-known that the Salvetti complex X_Γ is compact and non-positively curved, and its universal cover $\widetilde{X}_\Gamma$ is a CAT(0) cube complex. Moreover, right-angled Artin groups are CAT(0) groups; thus, they have at most quadratic Dehn functions. We refer to [11] for more details of these facts.

Fig. 2 Realator of the
Dicks–Leary presentation

Given a finite simplicial graph Γ, we define a group homomorphism $\phi : A_\Gamma \to \mathbb{Z}$ by sending all the generators of A_Γ to 1. The kernel of this homomorphism is called the *Bestvina–Brady group* defined by Γ, and is denoted by H_Γ. In fact, the map $\phi : A_\Gamma \to \mathbb{Z}$ is induced by $l : X_\Gamma \to S^1$, and the lift of l, denoted by $h : \widetilde{X}_\Gamma \to \mathbb{R}$ is a ϕ-equivariant Morse function; see [2], Theorem 5.12. Restricting the action of A_Γ on $\widetilde{X}_\Gamma$ to H_Γ, we obtain a geometric action of H_Γ on the zero level set $Z_\Gamma = h^{-1}(0)$.

The *flag complex* Δ_Γ on a finite simplicial graph Γ is a simplicial complex such that each complete subgraph K_n of Γ spans an $(n-1)$-simplex in Δ_Γ. When Δ_Γ is connected, H_Γ is finitely generated; when Δ_Γ is simply-connected, H_Γ is finitely presented; see [2] for the proof of these facts. When H_Γ is finitely presented, we can write down its *Dicks–Leary presentation* [12]:

Theorem 2.2 ([12], Corollary 3) *Let Γ be a finite simplicial oriented graph. Suppose that Δ_Γ is simply-connected. Then the Bestvina–Brady group H_Γ has the following finite presentation:*

$$H_\Gamma = \left\langle \overline{E}(\Gamma) \,\middle|\, ef = g = fe \text{ whenever } e, f, g \text{ form an oriented triangle} \right\rangle,$$

where $\overline{E}(\Gamma)$ is the set of oriented edges of Γ, and the oriented triangle is shown in Fig. 2

We will use the fact that H_Γ is finitely presented when Δ_Γ is simply-connected without specifying an orientation on Γ. We will give an orientation on Γ when we need to work with a finite presentation for H_Γ. The Dicks–Leary presentation can be reduced further:
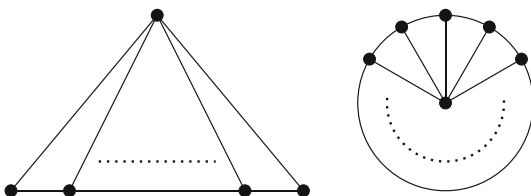
Corollary 2.3 ([15], Corollary 2.3) *If the flag complex on a finite simplicial graph Γ is simply-connected, then H_Γ has a presentation $H_\Gamma = F/R$, where F is the free group generated by the edges in a maximal tree of Γ, and R is a finitely generated normal subgroup of the commutator group $[F, F]$.*

While Dehn functions of right-angled Artin groups are at most quadratic, Dison [13] proved that Dehn functions of Bestvina–Brady groups are bounded above by quartic functions.

Theorem 2.4 ([13]) *Dehn functions of Bestvina–Brady groups are at most quartic.*

2.3 Interior dimensions

Let D be a triangulated disk. An *interior i-simplex* of D is an i-simplex whose faces do not intersect ∂D. We also call an interior 0-simplex an *interior vertex*, an interior 1-simplex an *interior edge*, and an interior 2-simplex an *interior triangle*. We say that D has *interior dimension d*, denoted by $\dim_I(D) = d$, if D contains interior d-simplices, and it has no interior k-simplices, $k > d$. If D contains no interior simplices, then we define $\dim_I(D) = 0$. We refer to Example 1.2 for concrete examples.

3 Disks with interior dimension 0

In this section, we prove the following theorem.

Theorem 3.1 *Let Γ be a finite simplicial graph. If Δ_Γ is a 2-dimensional triangulated disk satisfying $\dim_I(\Delta_\Gamma) = 0$, then $\delta_{H_\Gamma}(n) \simeq n^2$.*

For such a graph Γ, we will see later that the associated Bestvina–Brady group H_Γ has a graph-of-groups decomposition, where the edges groups are infinite cyclic groups; and the vertex groups are Bestvina–Brady groups on some induced subgraphs of Γ, namely, *fans* and *wheels*. Moreover, each of the vertex groups is isomorphic to a non-hyperbolic right-angled Artin group.

Recall that the *join* of two graphs Γ_1 and Γ_2, denoted by $\Gamma_1 * \Gamma_2$, is the graph obtained by taking the disjoint union of Γ_1 and Γ_2 together with all the edges that connect the vertices of Γ_1 and the vertices of Γ_2 (Fig. 3).

Definition 3.2 A *fan* $\mathcal{F}_{n+1}$ is the join of a vertex and a path P_n. A *wheel* $\mathcal{W}_{n+1}$ is the join of a vertex and a cycle C_n.

Remark 3.3 The flag complex on $\mathcal{W}_4$ is a tetrahedron, which is not 2-dimensional. Throughout this paper, unless otherwise stated, all the wheels have at least five vertices, that is, $\mathcal{W}_n$ for $n \geq 5$. Note that a triangle is also a fan $\mathcal{F}_3$.

Fans and wheels have a special structure: they can be decomposed as a join of a vertex and graph. When a finite simplicial graph Γ decomposes as a join $\Gamma = \{v\} * \Gamma'$, the Dicks–Leary presentation gives $H_\Gamma \cong A_{\Gamma'}$ (see Example 2.5 in [15]). That is, H_Γ is a right-angled Artin group. Thus, δ_{H_Γ} is at most quadratic.

Proposition 3.4 *Suppose a finite simplicial graph decomposes as a join $\Gamma = \{v\} * \Gamma'$. Then $H_\Gamma \cong A_{\Gamma'}$ and δ_{H_Γ} is at most quadratic. Moreover, if Γ' contains an edge, then $A_{\Gamma'}$ is non-hyperbolic and δ_{H_Γ} is quadratic.*

Proof Since $\Gamma = \{v\} * \Gamma'$, we have $A_\Gamma = \mathbb{Z} \times A_{\Gamma'}$. We claim that $H_\Gamma \cong A_{\Gamma'}$. Label the edges that have v as the common endpoint by $e_1, \ldots, e_k$; label the other end points of $e_1, \ldots, e_k$ by $v_1, \ldots, v_k$. Since $e_1, \ldots, e_k$ form a maximal tree of Γ, they generate H_Γ; see Corollary 2.3. Meanwhile, $v_1, \ldots, v_k$ generate $A_{\Gamma'}$. Define a map $\psi : H_\Gamma \to A_{\Gamma'}$ by sending e_i to v_i for $i = 1, \ldots, k$. This is a bijection between the generating sets of H_Γ and $A_{\Gamma'}$. We now argue that ψ preserves relators. Note that the relators of H_Γ and $A_{\Gamma'}$ are commutators. The generators e_i and e_j commute when they are two edges of the same triangle, that is, when their end points v_i and v_j are connected by an edge. Thus, v_i, v_j commute whenever e_i, e_j commute; the converse is true. Hence, ψ is an isomorphism.

Since $H_\Gamma \cong A_{\Gamma'}$ and $\delta_{A_{\Gamma'}}$ is at most quadratic, δ_{H_Γ} is at most quadratic. If Γ' contains an edge, then $H_\Gamma \cong A_{\Gamma'}$ contains $\mathbb{Z} \times \mathbb{Z}$ as a subgroup. Therefore, $H_{\Gamma'}$ cannot be hyperbolic and δ_{H_Γ} has to be quadratic.   □

Remark 3.5 In Proposition 3.4 Γ may have K_4 subgraphs. So there are infinitely many non-2-dimensional Bestvina–Brady groups whose Dehn functions are quadratic.

We want to point out that there are Bestvina–Brady groups that are not isomorphic to any right-angled Artin groups ([15], Proposition 9.4). The following corollary is an immediate consequence of Proposition 3.4.

Corollary 3.6 *If Γ is a fan or wheel, then δ_{H_Γ} is quadratic.*

Lemma 3.7 *Let Γ be a finite simplicial graph such that Δ_Γ is a 2-dimensional triangulated disk with $\dim_I(\Delta_\Gamma) = 0$. Then Γ can be represented as a tree T: each vertex of T represents a fan or a wheel; two vertices v, w of T are adjacent if the intersection of the graphs that are represented by v and w is an edge.*

Proof We observe that for any interior vertex of Δ_Γ, the induced subgraph on the interior vertex, together with its adjacent vertices, is a wheel. Also, note that if Δ_Γ has two interior vertices, then they are not connected. Otherwise, the edge that connects the two interior vertices would be an interior edge of Δ_Γ, which contradicts our assumption. Thus, there are three types of edges of Δ_Γ: (1) edges on $\partial\Delta_\Gamma$, (2) edges that connect interior vertices and vertices on $\partial\Delta_\Gamma$, and (3) edges that intersect $\partial\Delta_\Gamma$ at two vertices. Cutting along all the edges of type (3), we obtain connected components of Δ_Γ whose 1-skeletons are wheels and fans (triangles). For each connected component, we assign a vertex to it; two vertices are connected if the corresponding connected components intersect in Δ_Γ. Thus, we have the desire decomposition of Γ with an underlying graph T.

Now we show that T is a tree. Suppose T is not a tree, then T contains a circle C_n of length n. The flag complex on the subgraph of Γ whose decomposition corresponds to C_n would be a triangulated annulus. Thus, Δ_Γ would not be a triangulate disk, and this contradicts the assumption that Δ_Γ is a triangulated disk. Hence, T is a tree.   □

Note that the decomposition in Proposition 3.7 is not unique. Since for a fan $\mathcal{F}_{n+1}$, there are $p(n)$ such decompositions, where $p(n)$ is the partition function.

Let $\Gamma = \Gamma_1 \cup \Gamma_2$ be a finite simplicial graph. If $\Gamma_1 \cap \Gamma_2$ is a single edge, then the Bestvina–Brady group H_Γ splits over $\mathbb{Z}$ as $H_{\Gamma_1} *_\mathbb{Z} H_{\Gamma_2}$ by the Dicks–Leary presentation (see Theorem 2.2). It is not hard to see that Lemma 3.7 implies that H_Γ splits over $\mathbb{Z}$, and the vertex groups are CAT(0) groups. We summarize these statements in the following proposition.

Proposition 3.8 *Let Γ be a finite simplicial graph such that Δ_Γ is a triangulated disk with $\dim_I(\Delta_\Gamma) = 0$. Then H_Γ has a graph-of-groups decomposition, where the underlying graph is the tree T in Lemma 3.7, the edge groups are $\mathbb{Z}$, and the vertex groups are Bestvina–Brady groups defined by the graphs that are represented by the vertex of T in the Lemma 3.7. Moreover, the vertex groups are right-angled Artin groups, then hence, CAT(0) groups.*

To prove our main theorem in this section, we need the following proposition in [9]:

Proposition 3.9 ([9], Chapter II.11, 11.17 Proposition) *If each of the groups G_1 and G_2 is the fundamental group of a non-positively curved compact metric space, then so is $G_1 *_\mathbb{Z} G_2$. In particular, if G_1 and G_2 are CAT(0) groups, so is $G_1 *_\mathbb{Z} G_2$.*

Proof of Theorem 3.1 Let Γ be a finite simplicial graph such that Δ_Γ is a 2-dimensional triangulated disk with $\dim_I(\Delta_\Gamma) = 0$. By Proposition 3.8, H_Γ has a tree-of-groups decomposition, where the edge groups are $\mathbb{Z}$, and the vertex groups are CAT(0). Repeating Proposition 3.9 gives us that H_Γ is a CAT(0) group. Thus, δ_{H_Γ} is at most quadratic. Since Δ_Γ is a triangulated disk, H_Γ contains $\mathbb{Z} \times \mathbb{Z}$ subgroups, and thus, it is not hyperbolic. Therefore, δ_{H_Γ} is not linear. Hence, δ_{H_Γ} is quadratic.   □

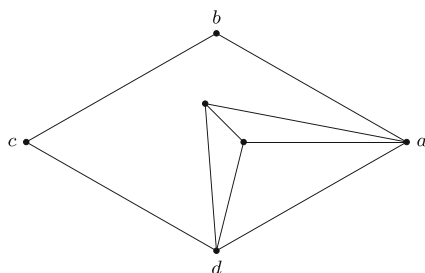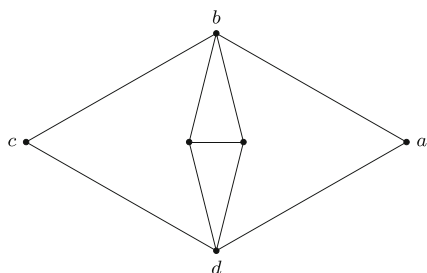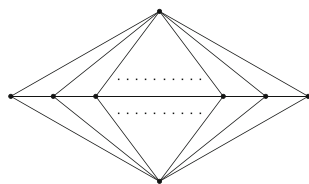**Fig. 4** The suspension of a path
of length at least 3

Fig. 5 An interior edge together with two vertices on $\partial\Delta_\Gamma$ form two adjacent triangles. These two vertices on $\partial\Delta_\Gamma$ are not adjacent, see the picture on the left. Otherwise, Γ would contain a K_4, see the picture on the right

4 Disks with square boundaries

The goal of this section is to prove the following:

Theorem 4.1 *Let Γ be a finite simplicial graph such that Δ_Γ is a 2-dimensional triangulated disk whose boundary is a square. If $\dim_I(\Delta_\Gamma) = d$ for $d \in \{0, 1, 2\}$, then $\delta_{H_\Gamma}(n) \cong n^{d+2}$.*

When $d = 0$, Theorem 4.1 is a corollary of Theorem 3.1. In Sect. 4.1, we establish the lower bound for δ_{H_Γ} for $d = 1, 2$. Since there is a universal quartic upper bound given by Dison [13], we only need to establish the cubic upper bound for δ_{H_Γ} for $d = 1$; the detailed proof is contained in Sect. 4.2. Before we proceed with the proof, we prove the following lemma which will be used later on.

Lemma 4.2 *Let Γ be a finite simplicial graph such that Δ_Γ is a 2-dimensional triangulated disk with square boundary. If $\dim_I(\Delta_\Gamma) = 1$, then Γ is the suspension of a path of length at least 3 (Fig. 4).*

Proof Define Γ' to be the graph whose edge set consists of all the interior edges of Δ_Γ. Label the four vertices on $\partial\Delta_\Gamma$ by a, b, c, d as shown in Fig. 5. Since Δ_Γ is a triangulated disk, each edge of Γ' together with two vertices on $\partial\Delta_\Gamma$ form two adjacent triangles, and these two vertices on $\partial\Delta_\Gamma$ are not adjacent. Otherwise, there would be a K_4 subgraph contained in Γ; see Fig. 5.

We make two claims on Γ'. The first claim is: Γ' has no vertices whose valency is greater than 3. Suppose Γ' has a vertex whose valency is greater than 3, that is, Γ' contains a tripod. Since each edge of the tripod together with two non-adjacent vertices on $\partial\Delta_\Gamma$, say b, d, form two adjacent triangles, there are two triangles in Δ_Γ share two consecutive edges; see Fig. 6. Thus, Γ is not a simplicial graph, we get a contradiction. Hence, no vertex of Γ' has valency greater than 3. This proves the first claim.

The second claim is that Γ' is a connected path. Suppose Γ' is not connected, say Γ' has k connected components $\Gamma'_1, \ldots, \Gamma'_k$. Since none of the vertices of Γ' has valency greater than

Fig. 6 The picture shows the simplest case: Γ' is a tripod, drown in thick lines. There are two edges connecting the central vertex of the tripod and the vertex d
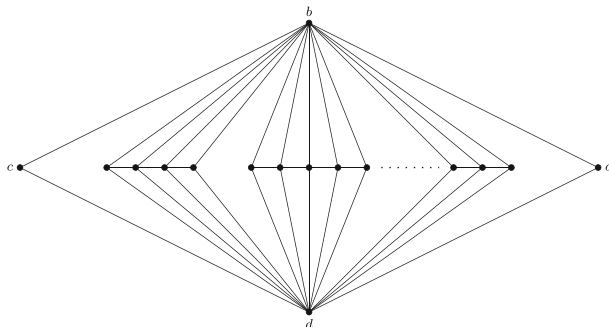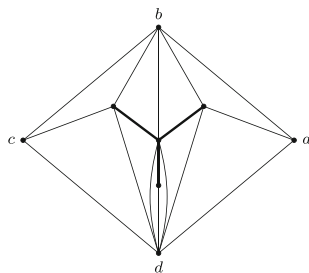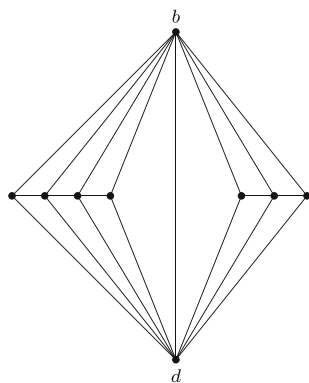

Fig. 7 Connected components of Γ'. Each pair of adjacent vertices of Γ' are connected to a pair of non-adjacent vertices on $\partial \Delta_\Gamma$

Fig. 8 Between Γ_i and Γ_{i+1}, vertices b, d are connected by an edge

3, each of $\Gamma'_1, \ldots, \Gamma'_k$ is a connected path. Also, all the pairs of adjacent vertices of Γ' are connected either to vertices a, c or vertices b, d simultaneously, say vertices b, d:

In Fig. 7, label from the left-most connected component to the right-most component of Γ' by $\Gamma'_1, \ldots, \Gamma'_k$, and define Γ_i to be the join of Γ'_i and $\{b, d\}$. Since Δ_Γ is a triangulated disk, there must be an edge connecting b and d between Γ_i and Γ_{i+1}, $i = 1, \ldots k - 1$:
In Fig. 8 we see that connecting b, d by an edge creates K_4 subgraphs in Γ. This contradicts our assumption. Thus, the graph Γ' is a connected path.

Now, we have shown that Γ' is a connected path, and all pairs of adjacent vertices of Γ' are connected either to vertices a, c or b, d simultaneously. Again, suppose b, d are connected to all vertices of Γ'. The two end vertices of Γ' have no choices but to be connected to a and c. Hence, Γ is a suspension of Γ'. This proves the lemma.   □

Remark 4.3 In [5], Brady gave an example of a cubic Dehn function δ_{H_Γ}, where Γ is the suspension of a path of length 3. Theorem 4.1 plus Lemma 4.2 gives a concrete family of graphs Γ satisfying $\delta_{H_\Gamma}(n) \simeq n^3$.

4.1 Lower bound

In [1], the authors introduced *height-pushing maps* to give a lower bound on the higher dimensional Dehn functions of *orthoplex groups*. The same technique can be used here to obtain the desired lower bound. We give necessary background here; see [1] for more details.

Let Γ be a finite simplicial graph. We use the notations X_Γ, $\widetilde{X}_\Gamma$, Z_Γ, h from Sect. 2.2. Recall that $\widetilde{X}_\Gamma$ is a CAT(0) cube complex. We put the ℓ^1-metric on each cube and extend it to the whole space $\widetilde{X}_\Gamma$. Let $B_r(x)$ and $S_r(x)$ be the ℓ^1-ball and ℓ^1-sphere in $\widetilde{X}_\Gamma$ centered at x with radius r, respectively.

A subspace $F \subseteq \widetilde{X}_\Gamma$ is called a *k-flat* if it is isometric to the Euclidean space $\mathbb{E}^k$.

Theorem 4.4 ([1], Theorem 4.2) *There is an H_Γ-equivariant retraction, called the* height-pushing map

$$\mathbf{P} : \widetilde{X}_\Gamma \setminus \bigcup_{v \notin Z_\Gamma} B_{1/4}(v) \to Z_\Gamma,$$

where the union is over the vertices that are not in Z_Γ, such that for all $t > 0$, when $\mathbf{P}$ is restricted to $h^{-1}([-t, t])$, $\mathbf{P}$ is a $(ct + c)$-Lipschitz map, where c is a constant which only depends on Γ.

In the next lemma, we establish the lower bound for δ_{H_Γ} in Theorem 4.1.

Lemma 4.5 *Let Γ be a finite simplicial graph such that Δ_Γ is a 2-dimensional triangulated disk with square boundary. If $\dim_I(\Delta_\Gamma) = d$, then $\delta_{H_\Gamma}(n) \succeq n^{d+2}$.*

We give the idea of the proof of Lemma 4.5. Recall that Bestvina–Brady groups H_Γ act geometrically on the zero level set $Z_\Gamma = h^{-1}(0)$. So the filling function of Z_Γ is equivalent to δ_{H_Γ}. For each r, we construct a loop S_r in Z_Γ whose length is $\simeq r$, and it bounds a disk in the ambient space $\widetilde{X}_\Gamma$ and a disk in Z_Γ. Then we use the height-pushing map to push the filling of the disk in $\widetilde{X}_\Gamma$ to get a lower bound of the filling of the loop S_r in Z_Γ.

Proof of Lemma 4.5 The case $d = 0$ follows from Theorem 3.1; the case $d = 2$ appears in [1]. We prove the case when $d = 1$ which uses the same strategy as the case $d = 2$. When $d = 1$, recall from Lemma 4.2 that Γ is the suspension of a path of length at least 3. Label the four vertices on the boundary of Δ_Γ as shown in Fig. 9.

Fig. 9 The square boundary of Δ_Γ and an interior 1-simplex σ
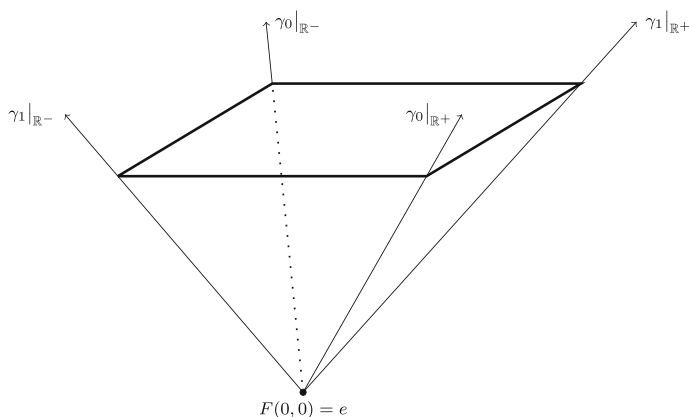
Fig. 10 The non-standard 2-dimensional flat $\overline{F}$. The parallelogram drown in the thick lines is the intersection $\overline{F} \cap h^{-1}(r)$

Define bi-infinite geodesic rays γ_i, $i = 0, 1$, in the 1-skeleton of $\widetilde{X}_\Gamma$:

$$\gamma_i(0) = e, \quad \gamma_i|_{\mathbb{R}^+} = a_i b_i a_i b_i \cdots, \quad \gamma_i|_{\mathbb{R}^-} = b_i a_i b_i a_i \cdots.$$

Define a map $F : \mathbb{Z} \times \mathbb{Z} \to A_\Gamma$ by

$$F(x) = \gamma_0(x_0)\gamma_1(x_1), \quad x = (x_0, x_1) \in \mathbb{Z} \times \mathbb{Z}.$$

The image of F consists of elements in the non-abelian group $\langle a_0, a_1, b_0, b_1 \rangle$. Let $\overline{F}$ be the non-standard 2-dimensional flat in $\widetilde{X}_\Gamma$ such that the set of its vertices is the image of F; see Fig. 10. Since

$$h(x) = h(F(x_0, x_1)) = |x_0| + |x_1|, \quad x = (x_0, x_1) \in \mathbb{Z} \times \mathbb{Z},$$

the flat $\overline{F}$ has a unique vertex $F(0, 0) = \gamma_0(0)\gamma_1(0) = e$ at height 0. We think of $\overline{F}$ as the boundary of a reversed infinite square pyramid with the apex $F(0, 0)$. For each $r > 0$, the intersection $\overline{F} \cap h^{-1}(r)$ is homeomorphic to S^1, which is a loop L_r at height r. This loop L_r bounds a 2-disk $\overline{F} \cap h^{-1}([0, r])$ in $\overline{F}$.

Using the group action A_Γ on $\widetilde{X}_\Gamma$, we translate the 2-disk $\overline{F} \cap h^{-1}([0, r])$ to $(a_0)^{-r}\overline{F} \cap h^{-1}([-r, 0])$. We denote the new 2-disk by D_r and its interior by $\mathring{D}_r$. The loop L_r at height r is translated to a loop S_r in Z_Γ that is also homeomorphic to S^1:

$$S_r := [(a_0)^{-r}\overline{F}] \cap h^{-1}(0) = [(a_0)^{-r}\overline{F}] \cap Z_\Gamma.$$

Notice that after performing this translation, the unique vertex $(a_0)^{-r}F(0, 0)$ is at height $-r$. Now we have that S_r is a loop in Z_Γ and it bounds a 2-disk D_r. The next step is to use the height-pushing map $\mathbf{P}$ to push this filling D_r of S_r in $\widetilde{X}_\Gamma$ to fill S_r in Z_Γ.

In order to use the height-pushing map, we need to do some surgery on D_r. At each vertex $v \in \mathring{D}_r$, replace $B_{1/4}(v)$ by a copy of Δ_Γ. We now show that after applying the height-pushing map to the surgered $\mathring{D}_r$, the scaled copies of 1-simplices in the interior of Δ_Γ at each vertex of the surgered $\mathring{D}_r$ do not intersect much in Z_Γ. We first consider two different 1-simplices σ_1 and σ_2 in the interior of Δ_Γ at a vertex v in $\mathring{D}_r$. Since σ_1 and σ_2 either are disjoint or intersect at a 0-simplex, the images $\mathbf{P}(\sigma_1)$ and $\mathbf{P}(\sigma_2)$ intersect at most at a 0-simplex. We next consider 1-simplices in the interior of Δ_Γ at different vertices v_1, v_2 in $\mathring{D}_r$. Let $\sigma = [x, y]$ be

an 1-simplex in the interior of Δ_Γ; see Fig. 9. Let v_1' and v_2' be vertices of the scaled copies $\mathbf{P}(\sigma)$ in Z_Γ, based at vertices v_1 and v_2 in $\mathring{D}_r$, respectively. Then we have

$$v_1' = (a_0)^{-r} v_1 x^{s_1} y^{t_1} \ \text{ and } \ v_2' = (a_0)^{-r} v_2 x^{s_2} y^{t_2}$$

for some $s_1, t_1, s_2, t_2 \in \mathbb{Z}_{\geq 0}$. If $v_1' = v_2'$, that is, the intersection of scaled copies $\mathbf{P}(\sigma)$ based at v_1 and v_2 is non-empty, then we have $v_1 = v_2$ since $\langle a_0, a_1, b_0, b_1 \rangle \cap \langle x, y \rangle = \{0\}$. Thus, no vertices of different scaled copies of σ are the same. That is, scaled copies of σ in Z_Γ are disjoint. Each interior 1-simplex is an intersection of two 2-simplices in Δ_Γ, so the image of the surgered $\mathring{D}_r$ under $\mathbf{P}$ has the area at least $2 \cdot |\{\text{number of 1-simplices}\}|$. Since we only need a lower bound, we don't need to count all the 1-simplices. For each vertex in $\mathring{D}_r$, we take one 1-simplex σ in Δ_Γ based at that vertex. As we have seen that the scaled copies $\mathbf{P}(\sigma)$ don't cancel out. So the filling of S_r in Z_Γ will be at least the sum of the length of these scaled copies $\mathbf{P}(\sigma)$. For each interior 1-simplex σ in Δ_Γ based at a vertex v of $\mathring{D}_r$, it follows by Theorem 4.4 that the length of the scaled copied $\mathbf{P}(\sigma)$ in Z_Γ grows linearly in terms of r, that is, the length of $\mathbf{P}(\sigma)$ depends on how far is σ pushed into Z_Γ by the height-pushing map. Thus, the further the σ is from Z_Γ, the longer the length of $\mathbf{P}(\sigma)$. At height $-r$, there is only one vertex in $\mathring{D}_r$, namely, the apex $(a_0)^{-r} F(0, 0)$. The image of the 1-simplex σ based at the apex under $\mathbf{P}$ is $cr + c$, by Theorem 4.4. At each height $i = -(r - 1), \ldots, -1$, there are $4i$ vertices and the image of 1-simplex σ under $\mathbf{P}$ has length $c(r - i) + c$. We have

$$\text{Area}(S_r) \geq (cr + c) + \sum_{i=1}^{r-1} 4i[c(r - i) + c] \simeq r^3.$$

Thus, the filling function of Z_Γ is at least cubic. Hence, δ_{H_Γ} is at least cubic. This proves the lemma.   □

4.2 Upper bound

As we mentioned at the beginning of this section, we only need to establish the cubic upper bound for $d = 1$ in Theorem 4.1. The proof relies on analyzing a van Kampen diagram of an arbitrary word $w \in H_\Gamma$ that represents the identity. All the van Kampen diagrams in this section are assumed to be minimal. The tool that we will be using is *corridor schemes*. Here we only give the definition; more details can be found in [4]. Let Γ be a finite simplicial graph with labelings on the edges such that Δ_Γ is a 2-dimensional triangulated disk. A *corridor scheme* for Γ is a collection τ of labeled edges of Γ such that every triangle of Δ_Γ has either zero or two edges in τ. Given a van Kampen diagram Δ, a τ-*corridor* is a corridor in Δ that consists of triangles; each triangle has exactly two edges in σ, and every pair of adjacent triangles intersect at an edge in σ. If α and β are two disjoint corridor schemes, then α-corridors and β-corridors never cross each other. If Γ is oriented, then each triangle in a diagram Δ is orientated.

Recalling the fact we only have to establish the cubic upper bound for $d = 1$ in Theorem 4.1 and Lemma 4.2, the graph Γ in the rest of this subsection will be the suspension of a path of length at least 3 with orientations and labels on the edges given by Fig. 11

The Dicks–Leary presentation (see Theorem 2.2) for H_Γ is $\langle \mathcal{A}, \mathcal{B}, \mathcal{X} | \mathcal{R} \rangle$, where

$$\begin{aligned}
\mathcal{A} &= \{a_1, \cdots, a_{k+1}\} \\
\mathcal{B} &= \{b_1, \cdots, b_{k+1}\} \\
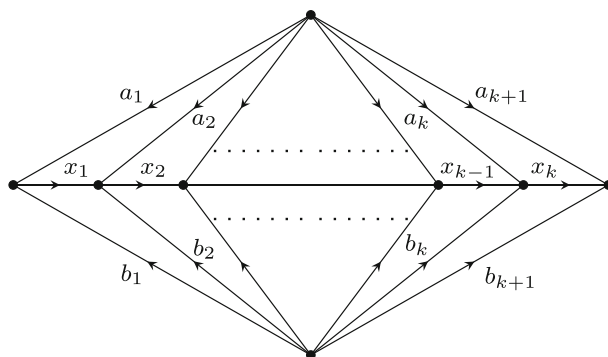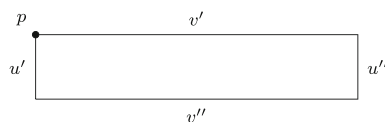\mathcal{X} &= \{x_1, \cdots, x_k\}
\end{aligned}$$

Fig. 11 The graph Γ with orientations and labels

Fig. 12 Boundary of a single corridor

$$\mathcal{R} = \{a_i x_i = a_{i+1} = x_i a_i, \ b_i x_i = b_{i+1} = x_i b_i\}, \ i = 1, \cdots, k$$

Let w be a freely reduced word of length at most n that represents the identity in H_Γ and Δ a minimal van Kampen diagram for w. Choose two disjoint corridor schemes $\alpha = \{a_1, \ldots, a_{k+1}\}$ and $\beta = \{b_1, \ldots, b_{k+1}\}$ for Γ. Note that α-corridors and β-corridors never cross each other. For each corridor in Δ, fix a vertex p of the corridor that is on $\partial \Delta$. When reading along the boundary of a corridor starting from p, we get a boundary word $u'v''u''v'$ or its cyclic permutation, where u', u'' are letters in α or β; v', v'' are words in the free group $F(x_1, \ldots, x_k)$. Note that u' and u'' are labelings of edges on $\partial \Delta$.

Remark 4.6 Since Γ is an oriented simplicial graph, all the corridors and triangles of a diagram Δ are oriented. For the pictures in the rest of this subsection, we omit the arrows on some of the edges for simplicity. Since each edge is labeled with a letter, and consecutive edges form a path, we don't distinguish letters and edges, and words and paths.

Definition 4.7 Let C_i, $1 \le i \le h$, be a corridor in Δ with the boundary word $u'_i v''_i u''_i v'_i$ (or its cyclic permutation) where u'_i, u''_i are letters in α or β; v'_i, v''_i are words in the free group $F(x_1, \ldots, x_k)$; see Fig. 12. If $u'_1, \ldots, u'_h$ and $u''_1, \ldots, u''_h$ are two sets of consecutive letters on $\partial \Delta$ and $v''_i = v'_{i+1}$ for $i = 1, \ldots h - 1$, then the subdiagram T of Δ obtained by gluing corridors $C_1, \ldots, C_h$ along the words $v''_1 = v'_2, \ldots, v''_{h-1} = v'_h$ is called a *stack*. The shorter word of the words v'_1 and v''_h is called the *top* of T; the longer word of the words v'_1 and v''_h is called the *bottom* of T. If v'_1 and v''_h have the same length, then we call either one the top and the other one the bottom. The words $u'_1 \cdots u'_h$ and $u''_1 \cdots u''_h$ are called the *legs* of T, and the number h is called the *height* of T.

Remark 4.8 For two consecutive corridors C_i and C_{i+1} as defined in the Definition 4.7, every 2-cell of Δ with an edge labeled with a letter in the word $v''_i = v'_{i+1}$ must be part of either C_i or C_{i+1}. Otherwise, it would violate the minimality assumption on Δ.

Roughly speaking, a stack is a pile of corridors where one corridor sits on top of another. Note that the top and bottom of a stack are not parts of $\partial \Delta$, and they might have different
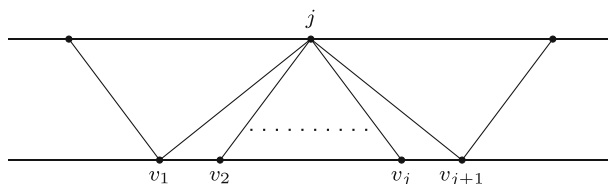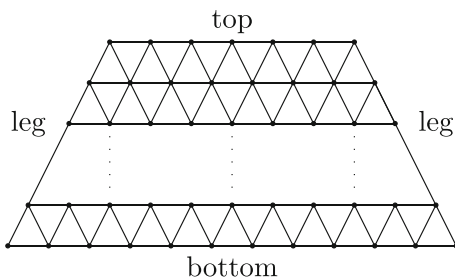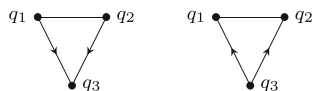
lengths; the legs are parts of $\partial\Delta$, and they are not necessarily straight. Figure 13 shows an example of a stack. For simplicity, we draw a stack with straight legs.

Definition 4.9 Let C be either a single α-corridor or β-corridor with boundary word $u'v''u''v'$ (or its cyclic permutation), as shown in Fig. 12. We say that a vertex q on the boundary of C labeled by the word v' (respectively v'') is a j-vertex, or q has type j, if there are $j+1$ edges connecting q to $j+1$ distinct consecutive vertices on the part of boundary of C labeled by the word v'' (respectively v'); see Fig. 14.

We say that a pair of adjacent vertices q_1 and q_2 on the boundary of C labeled by the word v' (respectively v'') *generate* a vertex q_3 in v'' (respectively v') if there is a triangle shown as Fig. 15.

Lemma 4.10 *Let Γ be the graph as shown in Fig. 11. Let $w \in H_\Gamma$ be a freely reduced word that represents the identity. Let T be a stack in a minimal van Kampen diagram Δ for w such that the top of T has length l and the height of T is h. Then the area of T satisfies*

$$Area(T) \le K(lh^2 + h^3),$$

where K is a positive constant that does not depend on l and h.

The proof of Lemma 4.10 relies on a series of lemmas that analyze the boundaries of corridors of a stack. Since all the van Kampen diagrams are assumed to be minimal, in Lemma 4.10 each vertex on the boundary of a corridor is of type at most k for a fixed $k \ge 3$. We label the boundary words of corridors of a stack T as shown in Fig. 16:

Let's look at a single corridor C_i as shown in Fig. 17:

Each edge x_m of t_i, $1 \le m \le k$, is a part of the boundary of a triangle in the interior of C_i; see Fig. 18.

Depending on C_i is an α-corridor or β-corridor, the orientation of x_m, and the orientation of u_i', u_i'' (they have the same orientation), we have the following eight possibilities:

Fig. 16 Boundary words of corridors in a stack T

Fig. 17 A single corridor with boundary words

Fig. 18 A 2-cell in a corridor
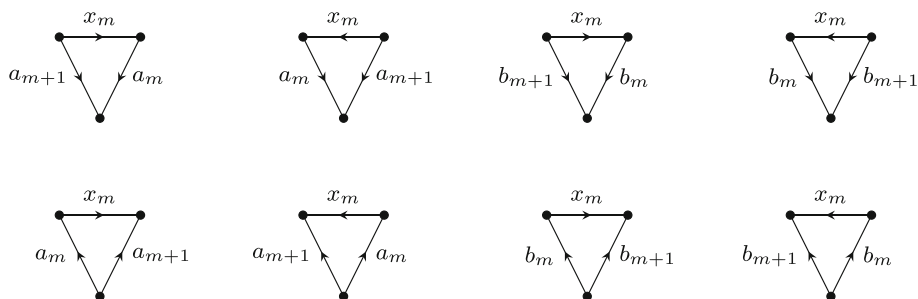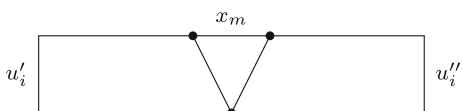

Fig. 19 The first row shows the cases where the arrows on u_i' and u_i'' are pointing from t_i to t_{i+1}; the second row shows the cases where the arrows on u_i' and u_i'' are pointing from t_{i+1} to t_i. The left two columns are the cases where C_i is an α-corridor; the right two columns are the cases where C_i is a β-corridor
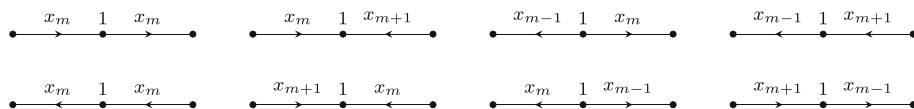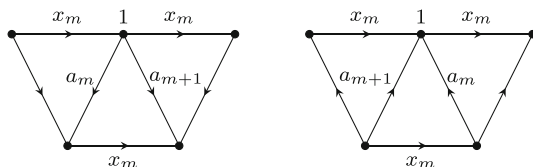
Fig. 20 Possible combinations of edges that create 1-vertices

Fig. 21 Two choices to complete a triangle

Note that the boundary word of each triangle in Fig. 19 is a relator of H_Γ.

Lemma 4.11 *Let C_i be either an α-corridor or β-corridor in a stack T as shown in Figs. 16 and 17.*

(1) *The area of C_i is $|t_i| + |t_{i+1}|$.*
(2) *Suppose $|t_i| < |t_{i+1}|$, then*

$$|t_{i+1}| = \sum_j j \cdot \left|\{\ j\text{-vertices on } t_i\}\right|.$$

Proof (1) Since each edge on t_i and t_{i+1} is part of a unique triangle in C_i, the result follows.
(2) Since each j-vertex on t_i contributes j edges on t_{i+1}, the statement follows immediately. □

Lemma 4.12 *Let C_i be either an α-corridor or β-corridor in a stack T as shown in Figs. 16 and 17. There are eight combinations of edges on t_i (respectively t_{i+1}) that will create 1-vertices on the t_i (respectively t_{i+1}) for a given m, $2 \le m \le k - 1$, as shown in Fig. 20.*

Proof We prove the case when C_i is an α-corridor; the case for a single β-corridor is similar. To see the conclusion, we only need to know how to fill C_i. Take the left-most picture in the first row of Fig. 20. Suppose the x_m's are edges on either t_i or t_{i+1}. By Fig. 19, we have two choices to complete the triangles based on the x_m's; see Fig. 21.
Thus, the vertex is a 1-vertex. The arguments for other combinations are similar. □

Lemma 4.13 *Let C_i and C_{i+1} be two consecutive corridors in a stack T. Suppose that the arrows on the edges u_i', u_i'', u_{i+1}', u_{i+1}'' have the same orientation, as shown in Fig. 22. Assume that there are no 0-vertices on t_i. Then*

(1) *All the vertices on t_{i+1} are 1-vertices, 2-vertices, or 3-vertices, except possibly the two vertices at the ends of t_{i+1}.*
(2) *All the vertices on t_{i+2} are either 1-vertices or 2-vertices, except possibly the two vertices at the ends of t_{i+1}.*
(3) *We have $|t_i| \le |t_{i+1}| \le |t_{i+2}|$.*

Proof We prove the lemma for the case when C_i, C_{i+1} are consecutive α-corridors, and the arrows on u_i', u_i'', u_{i+1}', u_{i+1}'' are pointing away from t_i. Other cases are similar.
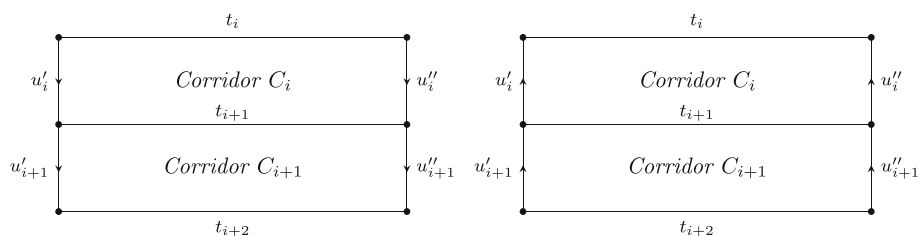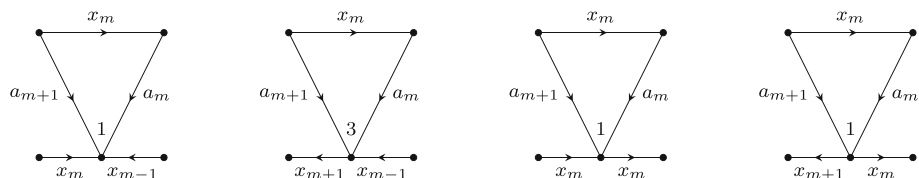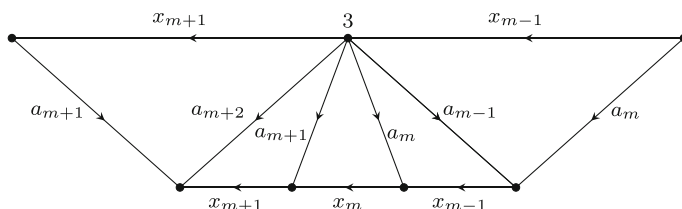
Fig. 22 Two consecutive corridors

Fig. 23 A pair of adjacent vertices on t_i generates either a 1-vertex or 3-vertex on t_{i+1}

Fig. 24 A 3-vertex

(1) We claim that every pair of adjacent vertices on t_i generates either a 1-vertex or 3-vertex on t_{i+1}. Let two adjacent vertices on t_i be connected by an edge x_m. These two adjacent vertices generate a vertex on t_{i+1}; Fig. 23 lists all possible combinations of edges that meet at the vertex on t_{i+1} that is generated by a pair of adjacent vertices on t_i.

The 1-vertices in Fig. 23 are recognized by Lemma 4.12. The following picture shows that the vertex in Fig. 23 is a 3-vertex; see Fig. 24.

There are four more cases obtained by flipping the pictures in Fig. 23 such that the arrow on the edge x_m of t_i has the opposite orientation. This proves the claim.

Next, we show that the vertices on t_{i+1} that are not generated by pairs of adjacent vertices on t_i are 2-vertices, except the two vertices at the end of t_{i+1}. We claim that each j-vertex on t_i creates $j-1$ vertices on t_{i+1} that are all 2-vertices. For any j-vertex on t_i (respectively t_{i+1}), by definition, there are $j+1$ edges connecting the j-vertex to $j+1$ consecutive distinct vertices on t_{i+1} (respectively t_i). That is, there are j distinct triangles based on j consecutive edges on t_{i+1} (respectively t_i) that has the j-vertex as the common vertex; see Fig. 25. Let x_{r-1}, x_r be two consecutive edges, $r \in \{m, \dots, m+j-1\}$, and let the vertex v_r be the common vertex of x_{r-1} and x_r. Figure 26 shows that v_r is a 2-vertex. This proves the claim.

(2) We have shown that all the vertices on t_{i+1} are 1-vertices, 2-vertices, or 3-vertices. Each of the vertices on t_{i+1} creates numbers of 0, 1, or 2 vertices on t_{i+2}, respectively, and they are all 2-vertices. Other vertices on t_{i+2} are generated by pairs of adjacent vertices on t_{i+1}. We now show that these vertices on t_{i+2} are 1-vertices. We prove the claim by showing all the possible combinations of types of vertices on t_{i+1}. We have six cases: pairs of
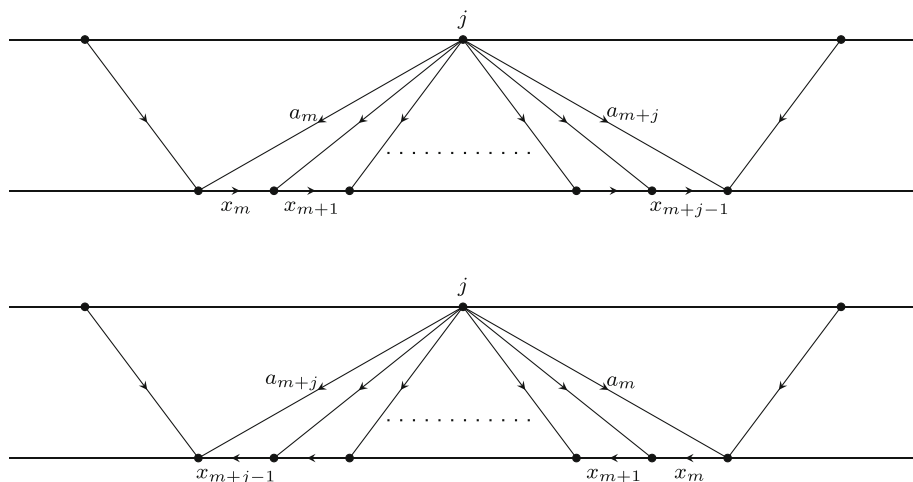
Fig. 25 Each j-vertex on t_i (respectively t_{i+1}) creates $j - 1$ vertices on t_{i+1} respectively t_i) that are all 2-vertices
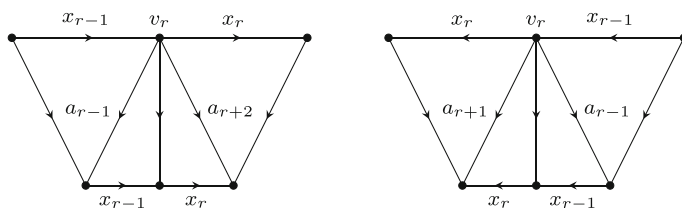

Fig. 26 The vertex v_r on t_{i+1} is a 2-vertex

adjacent 1-vertices, adjacent 2-vertices, and adjacent 3-vertices; pairs of adjacent 1-vertex and 2-vertex; pairs of adjacent 1-vertex and 3-vertex; and pairs of adjacent 2-vertex and 3-vertex. In the following pictures, all the 1-vertices are recognized by Lemma 4.12.

Figure 27 shows that a pair of adjacent 1-vertices on t_{i+1} generates a 1-vertex on t_{i+2}:

Next, Fig. 28 shows that a pair of adjacent 1-vertex and 2-vertex on t_{i+1} generates a 1-vertex on t_{i+2}. Recall that Figs. 23 and 26 are the only situations of 1-vertex and 2-vertex on t_{i+1}.

For a pair of adjacent 2-vertices on t_{i+1}, we have one combination up to orientation; see Fig. 29.

For a pair of adjacent 1-vertex and 3-vertex on t_{i+1}, we have (Fig. 30):

For a pair of adjacent 2-vertex and 3-vertex on t_{i+1}, since the number of combinations of edges on t_{i+1} that will create 2-vertices and 3-vertices are limited, we have fewer cases here (Fig. 31):

Finally, for a pair of adjacent 3-vertices, we have only one possibility up to orientation; see Fig. 32.

(3) Since we assume that there are no 0-vertices on t_i, the number of vertices on t_{i+1} is no less than the number of vertices on t_i, and the number of vertices on t_{i+2} is also no less than the number of vertices on t_{i+1}. Thus, we have

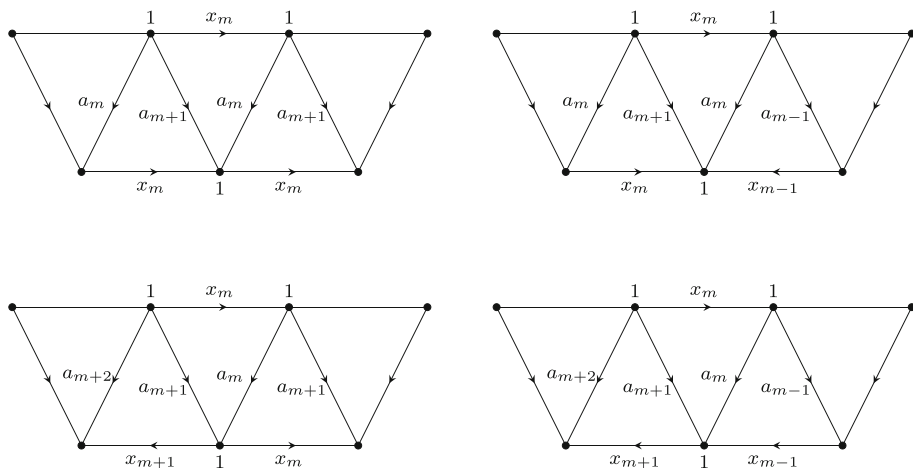$$|t_i| = (\text{number of vertices on } t_i) - 1$$

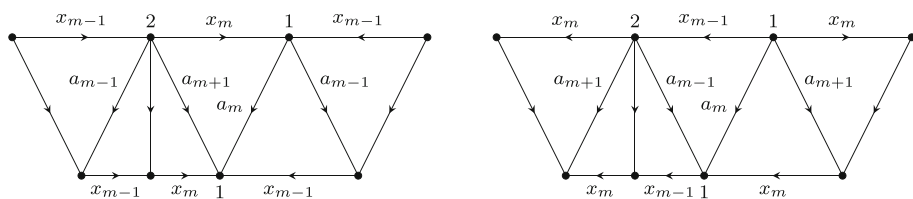**Fig. 27** Two adjacent 1-vertices on t_{i+1} generate a 1-vertex on t_{i+2}

Fig. 28 A pair of adjacent 1-vertex and 2-vertex on t_{i+1} generates a 1-vertex on t_{i+2}

Fig. 29 A pair of adjacent 2-vertices on t_{i+1} generates a 1-vertex on t_{i+2}
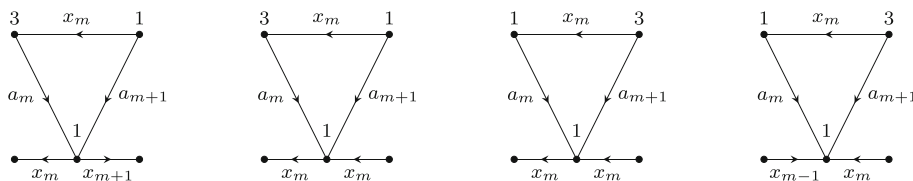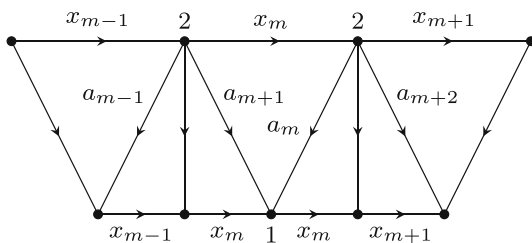

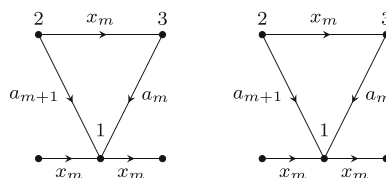**Fig. 30** A pair of adjacent 1-vertex and 3-vertex on t_{i+1} generates a 1-vertex on t_{i+2}

Fig. 31 A pair of adjacent 2-vertex and 3-vertex on t_{i+1} generates a 1-vertex on t_{i+2}

Fig. 32 A pair of adjacent
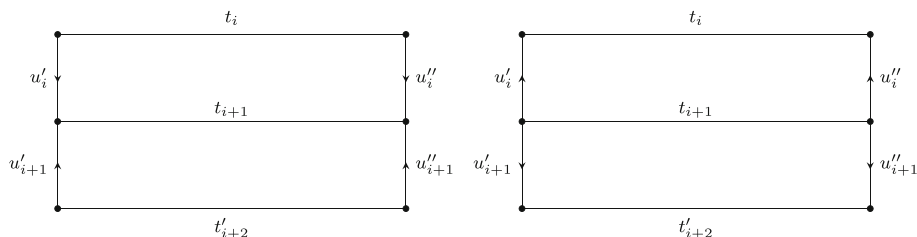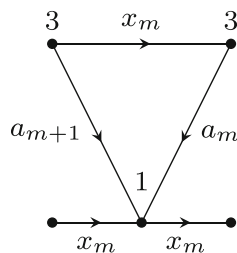3-vertex on t_{i+1} generates a
1-vertex on t_{i+2}

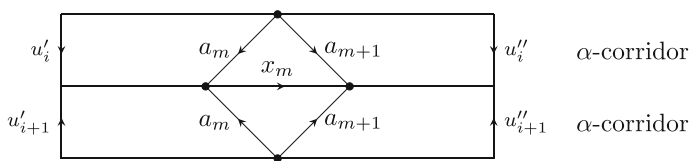**Fig. 33** Edges u_i', u_i'' and u_{i+1}', u_{i+1}'' have different orientations

Fig. 34 Two triangles from different α-corridors with opposite orientations

$$\leq (\text{number of vertices on } t_{i+1}) - 1$$
$$= |t_{i+1}|$$

and

$$|t_{i+1}| = (\text{number of vertices on } t_{i+1}) - 1$$
$$\leq (\text{number of vertices on } t_{i+2}) - 1$$
$$= |t_{i+2}|.$$

Hence, $|t_i| \leq |t_{i+1}| \leq |t_{i+2}|$.

$\square$

Lemma 4.14 *Let C_i and C_{i+1} be two consecutive corridors in a stack T as in the Lemma 4.13. Let the arrows on the edges labeled by u_i', u_i'' and u_{i+1}', u_{i+1}'' have different orientations. There are two cases, as shown in Fig. 33. Assume that there are no 0-vertices on t_i. Then $|t_{i+2}'| \leq |t_{i+2}|$, where t_{i+2} is in Fig. 22.*

Proof We prove the case when u_i', u_i'', u_{i+1}', u_{i+1}'' are pointing toward t_{i+i}. The other case is similar. We claim that in this case, C_i and C_{i+1} cannot be both α-corridors or β-corridors. Suppose C_i and C_{i+1} are both α-corridors (respectively β-corridors), then there are two triangles that share a unique common edge on t_{i+1}:
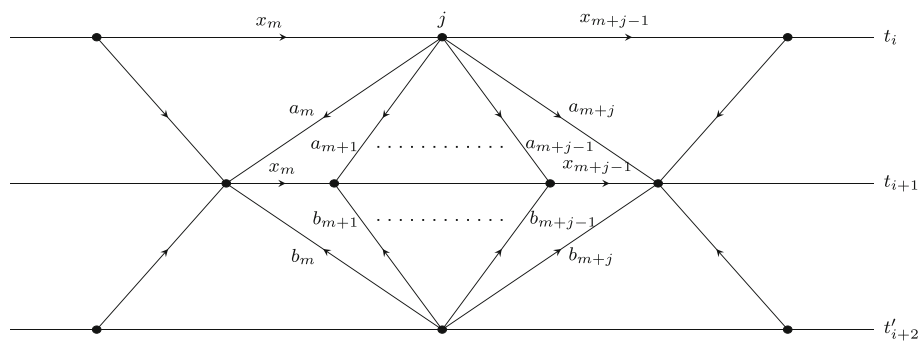
Fig. 35 Every pair of adjacent vertices of the distinct $j + 1$ vertices on t_{i+1} generates the same vertex on t'_{i+2}

The situation as shown in Fig. 34 contradicts the fact that T is part of a minimal van Kampen diagram since we can obtain a smaller van Kampen diagram by canceling these two triangles. This proves the claim.

Now suppose C_i is an α-corridor and C_{i+1} is a β-corridor. By definition, each j-vertex on t_i is adjacent to $j + 1$ consecutive distinct vertices on t_{i+1}:
From Fig. 35 we see that every pair of adjacent vertices of these $j + 1$ consecutive distinct vertices on t_{i+1} generates the same vertex on t'_{i+2} since C_{i+1} is a β-corridor. That is, each j-vertex on t_i creates $j - 1$ vertices on t_{i+1} and they are 0-vertices. It follows that the number of vertices on t'_{i+2} is less than the numbers of vertices on t_{i+2} in Lemma 4.13. Thus, we have

$$
\begin{aligned}
|t'_{i+2}| &= (\text{number of vertices on } t'_{i+2}) - 1 \\
&\leq (\text{number of vertices on } t_{i+2}) - 1 \\
&= |t_{i+2}|.
\end{aligned}
$$

This completes the proof.   □

Now, we prove Lemma 4.10.

Proof of Lemma 4.10. Let T be a stack with labelings as shown in Fig. 16. Recall that $t_0, \ldots, t_h$ are words in the free group $F(x_1, \ldots, x_k)$ and u'_i, u''_i are both letters either in the corridor scheme $\alpha = \{a_1, \ldots, a_{k+1}\}$ or $\beta = \{b_1, \ldots, b_{k+1}\}$. Since the area of a stack T is the sum of the areas of the corridors that contained in T, by Lemma 4.11 we have

$$\text{Area}(T) = |t_0| + 2|t_1| + \cdots + 2|t_{h-1}| + |t_h| \leq 2\left(|t_0| + \cdots + |t_h|\right).$$

Thus, upper bounds on $|t_0|, \ldots, |t_n|$ give an upper on Area(T). In order to obtain an upper bound on $|t_i|$, we need a few assumptions. Recall that for a fixed k, each vertex of T is at most a k-vertex. The assumptions we need here are

(1) the vertices on t_0 and the two vertices at the two ends of t_i are k-vertices;
(2) the arrows on $u'_i, u''_i, i = 1, \ldots, h$, are pointing away from t_0 (Lemma 4.13 and Lemma 4.14).

The first assumption gives us an upper bound on $|t_0|$. From Lemma 4.11 we know that the length of t_{i+1} depends on the types of the vertices on t_i. The second assumption ensures that $|t_i| \leq |t_{i+1}| \leq |t_{i+2}|$. We compute $|t_i|$ as follows.

For $|t_1|$, since $|t_0| = l$ and all the vertices on t_0 are k-vertex, we have $|t_1| = k(l + 1)$.

On t_1, there are two k-vertices at the two ends. Lemma 4.13 tells us that every pair of adjacent vertices on t_0 generates either a 1-vertex or a 3-vertex on t_1, but we may assume that they are all 3-vertices so that we can get the largest possible $|t_2|$. So the number of 3-vertices on t_1 is l; other vertices on t_1 are 2-vertices and there are $(k-1)(l+1)$ of them. Knowing the types of vertices on t_1 gives the length of t_2:

$$|t_2| = 2 \cdot k + l \cdot 3 + (k-1)(l+1) \cdot 2 = 2kl + l + 4k - 2$$

For $i \geq 2$, every pair of adjacent vertices on t_{i-1} generates a 1-vertex on t_i by Lemma 4.13, so the number of 1-vertices on t_i is $|t_{i-1}|$. Every 2-vertex on t_{i-1} creates a 2-vertex on t_i and the two k-vertices at the ends of t_{i-1} creates $(k-1)$ 2-vertices on t_i. So the number of 2-vertices on t_i is the number of 2-vertices on t_{i-1} plus $2(k-1)$:

$$(kl + l + k - 1) + (i-1) \cdot 2(k-1) = kl + l + (2i-1)k - 2i + 1.$$

Having the information of the vertices on t_i we get

$$\begin{aligned} |t_{i+1}| &= |t_{i-1}| \cdot 1 + [kl + l + (2i-1)k - 2i + 1] \cdot 2 + 2 \cdot k \\ &= |t_{i-1}| + 2kl + 2l + 4ik - 4i + 2 \end{aligned}$$

for $i = 2, \ldots, h-1$. Let

$$d(i) = |t_{i+1}| - |t_{i-1}| = 2kl + 2l + 4ik - 4i + 2, \quad i = 2, \ldots, h-1,$$

then $\{d(i)\}$ is an arithmetic sequence whose difference is $4k - 4$ and

$$d(i+2) - d(i) = 8k - 8.$$

When i is even, we have

$$\begin{aligned} |t_{i+1}| &= |t_1| + d(2) + d(4) + \cdots + d(i) \\ &= |t_1| + \frac{i}{2}d(2) + i(i-2)(k-1), \end{aligned}$$

and when i is odd, we have

$$\begin{aligned} |t_{i+1}| &= |t_2| + d(3) + d(5) + \cdots + d(i) \\ &= |t_2| + \left(\frac{i-1}{2}\right)d(3) + (i-1)(i-3)(k-1). \end{aligned}$$

When h is odd, we have

$$\text{Area}(T) \leq 2\sum_{i=1}^{h} |t_i| = 2\left(|t_0| + |t_1| + |t_2| + \sum_{\substack{i=2 \\ i \text{ is even}}}^{h-1} |t_{i+1}| + \sum_{\substack{i=3 \\ i \text{ is odd}}}^{h-2} |t_{i+1}| \right).$$

Furthermore,

$$\begin{aligned} \sum_{\substack{i=2 \\ i \text{ is even}}}^{h-1} |t_{i+1}| &= \sum_{\substack{i=2 \\ i \text{ is even}}}^{h-1} \left[|t_1| + \frac{i}{2}d(2) + i(i-2)(k-1) \right] \\ &\leq h|t_1| + [d(2) - 2(k-1)]h^2 + (k-1)h^3 \\ &\leq 12klh^2 + kh^3. \end{aligned}$$

and

$$\sum_{\substack{i=3\\ i \text{ is odd}}}^{h-2} |t_{i+1}| = \sum_{\substack{i=3\\ i \text{ is odd}}}^{h-2} \left[|t_2| + \left(\frac{i-1}{2}\right) d(3) + (i-1)(i-3)(k-1) \right]$$

$$\leq h|t_2| + d(3)h^2 + kh^3 + kh^2 + 2h$$

$$\leq 24klh^2 + kh^3.$$

Thus,

$$\text{Area}(T) \leq 2 \left[|t_0| + |t_1| + |t_2| + (12klh^2 + kh^3) + (24klh^2 + kh^3) \right]$$

$$\leq 92k(h^3 + lh^2).$$

When h is even, the computation is similar. Hence, $\text{Area}(T) \leq K(h^3 + lh^2)$, where K is a positive constant which does not depend on l and h. □

Lemma 4.15 *Let Γ be the graph as shown in Fig. 11. Then $\delta_{H_\Gamma}(n) \preceq n^3$.*

Proof Let w be a freely reduced word of length at most n that represents the identity in H_Γ. Let Δ be a minimal van Kampen diagram for w. Choose corridor schemes $\alpha = \{a_1, \ldots, a_{k+1}\}$ and $\beta = \{b_1, \ldots, b_{k+1}\}$ for Γ, then the van Kampen diagram Δ consists of stacks, $T_1, \ldots, T_m$. Denote the two legs of T_i by U_i' and U_i'', and the height of T_i by $|U_i'| = |U_i''| = h_i$, $i = 1, \ldots, m$. Note that U_i' and U_i'' are words on $\partial\Delta$ that consist of letters in the corridor schemes α and β. The boundary word w is a cyclic permutation of the following word, and we also denoted it by w:

$$w = A_1 B_1 A_2 B_2 \cdots A_r B_s,$$

where each of the words $A_1, \ldots, A_r$ consists of one or more words from $U_1', \ldots, U_m'$ and $U_1'', \ldots, U_m''$; each of the words $B_1, \ldots, B_s$ is a word in the free group $F(x_1, \ldots, x_k)$. The length of each of the words $A_1, \ldots, A_r$ is either the height of a single stack or the sum of the heights of multiple stacks; each of the words $B_1, \ldots, B_s$ is a base of a stack or part of a base of a stack. Denote the length of the words $B_1, \ldots, B_s$ by $l_1, \ldots, l_s$, respectively. Let

$$h = |A_1| + \cdots + |A_r| = 2(h_1 + \cdots + h_m) = 2\sum_{i=1}^{m} h_i$$

and

$$l = |B_1| + \cdots + |B_s| = \sum_{i=1}^{s} l_i.$$

Consider a stack T' whose top is the word $B_1 \cdots B_s$ of length l and whose legs are $U_1' \cdots U_m'$ and $U_1'' \cdots U_m''$ and the height $h = |U_1' \cdots U_m'| = |U_1'' \cdots U_m''|$, assuming that all the the arrows on U_i', U_i'' are pointing away from the top; see Fig. 36.

There are three possible cases that the van Kampen diagram Δ could be. The first case is that every stack has a base that is part of $\partial\Delta$, as shown in Fig. 37. The second case is that every stack has a base that is either on $\partial\Delta$, or part of it is on $\partial\Delta$, as shown in Fig. 38. The third case is that there is a stack whose bases are not part of $\partial\Delta$, as shown in Fig. 39. We show that $\text{Area}(\Delta) \leq \text{Area}(T')$ in each of these three cases.

Case 1 Recall that each of A_i is a leg of one or more stacks; each B_i is part of a base of a stack or a base of a stack. By assumption, each stack T_i has a base that is on $\partial\Delta$, say
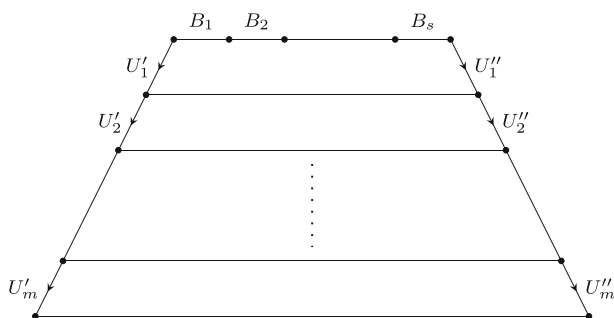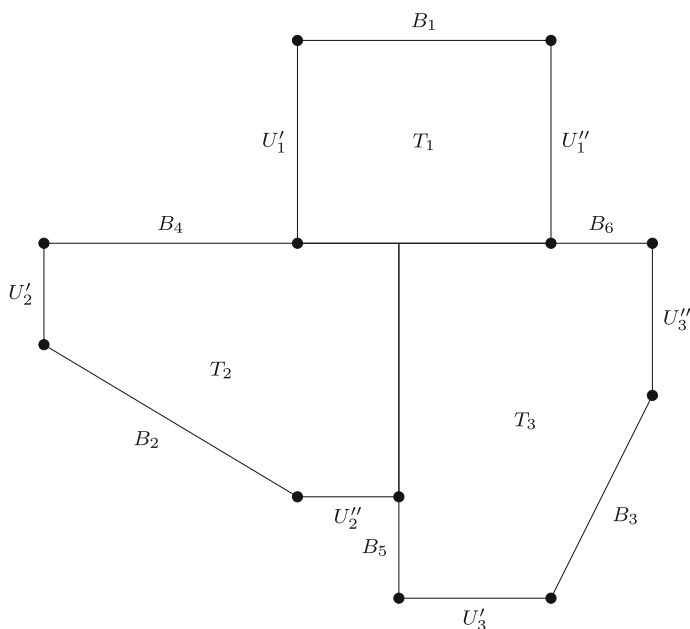
Fig. 36 The stack T'

Fig. 37 *Case 1* Every stack T_i has a base B_i that is part of $\partial\Delta$

B_i is a base of the stack T_i. If B_i is the top of the stack T_i, then the top of the stack T_i' in Fig. 40 is longer than B_i. Thus, Area(T_i) $\leq$ Area(T_i'). If B_i is the bottom of the stack T_i, then consider a stack whose heights are U_i', U_i'' and whose top is B_i. The area of this stack is obviously greater than the area of T_i, but less than the area of T_i' in Fig. 40. Thus, for each stack T_i, $i = 1, \ldots, m$, there is a stack T_i' in T' satisfying Area(T_i) $\leq$ Area(T_i'). These substacks $T_1', \ldots, T_m'$ are disjoint inside T' because their legs are disjoint. Each substack T' is at different height inside T', as shown in Fig. 40:

We have

$$\begin{aligned}
\text{Area}(w) &= \text{Area}(\Delta) \\
&= \text{Area}(T_1) + \cdots + \text{Area}(T_m) \\
&\leq \text{Area}(T_1') + \cdots + \text{Area}(T_m')
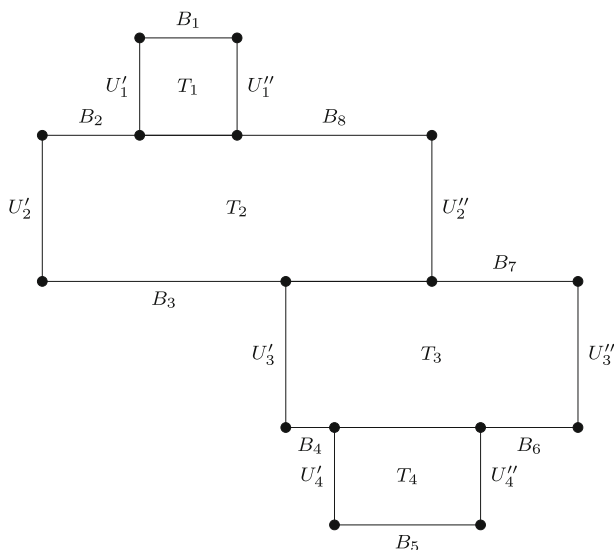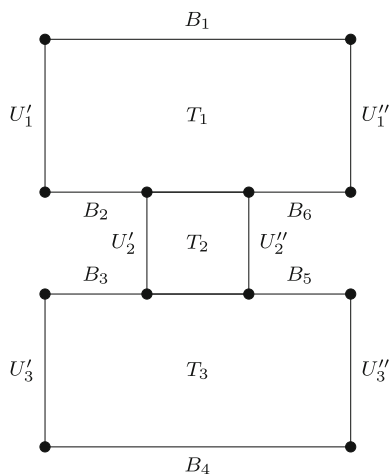\end{aligned}$$

Fig. 38 *Case 2* At least one of the stacks such that part of its bases is part of $\partial\Delta$

Fig. 39 *Case 3* At least one of the stacks whose bases are not part of $\partial\Delta$

$$\leq \text{Area}(T')$$
$$\leq C(h^3 + lh^2)$$
$$\leq 2Cn^3$$

for some positive constant C, which does not depend on $|w| = n$. The second last inequality follows by Lemma 4.10, and the last inequality holds since $l \leq n$ and $h \leq n$. Thus, we prove the claim for the first case.

Case 2 Suppose that the van Kampen diagram Δ has some stacks whose bases are not all on $\partial\Delta$, as shown in Fig. 38. Divide those stacks into smaller stacks as following:
In Figure 41, each of the stacks $\overline{T}_i$ has at least one base $\overline{B}_i$ that is on $\partial\Delta$. Thus, Case 2 follows by Case 1.
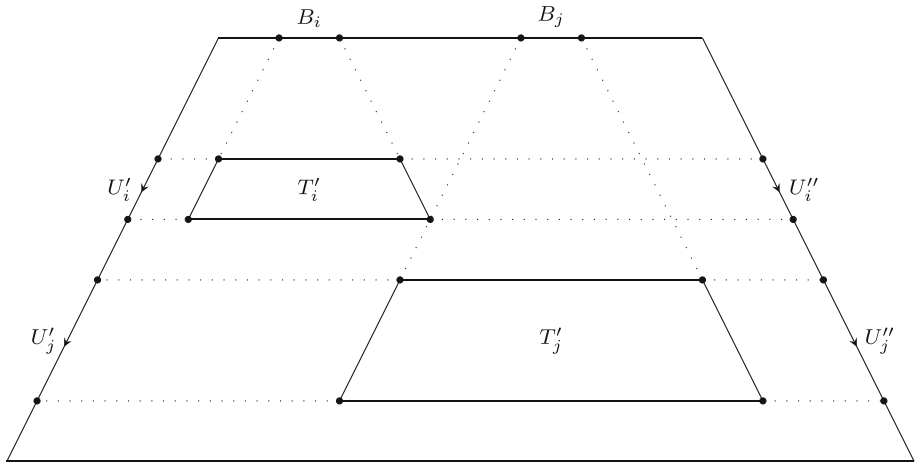
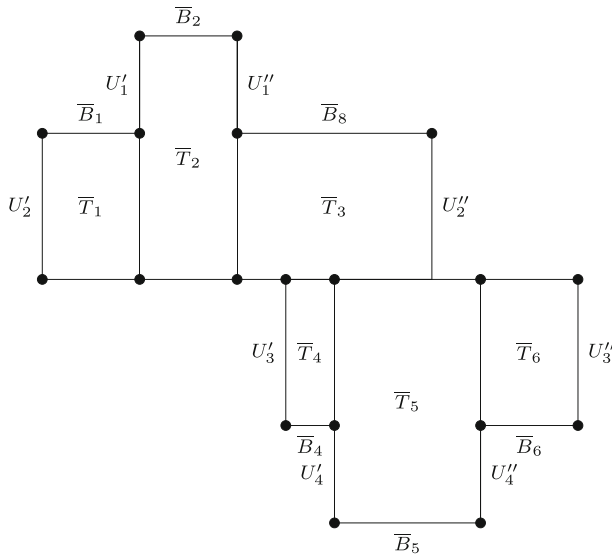**Fig. 40** Disjoint substacks T_i' and T_j' in T'

Fig. 41 A van Kampen diagram in Case 2

Case 3 Suppose that there is a stack in Δ whose bases are not on $\partial\Delta$, as shown in Fig. 39. Divide Δ and rearrange the stacks as follows:
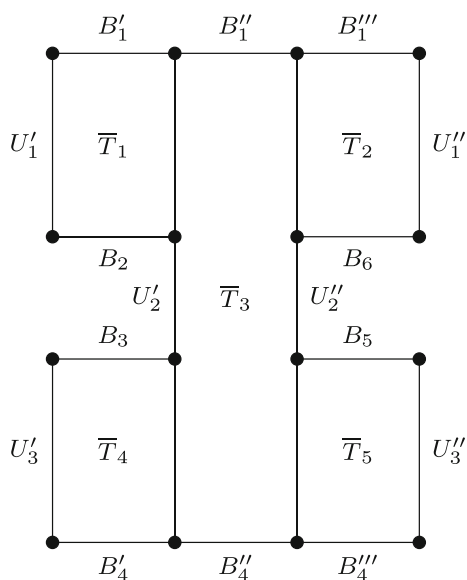
Again, all the stacks in Fig. 42 have a base that is on $\partial\Delta$. Thus, Case 3 follows by Case 1.

This completes the proof of the lemma.   □

5 Graphs with K_4 subgraphs

In the previous sections, we considered finite simplicial graphs Γ that do not contain K_4 subgraphs. In this section, we consider finite simplicial graphs that can contain K_4 subgraphs.

Fig. 42 A van Kampen diagram in Case 3

The main difference is that the flag complexes on finite simplicial graphs with K_4 subgraphs are not 2-dimensional.

Unfortunately, we have not been able to characterize the Dehn function δ_{H_Γ} when Δ_Γ is not 2-dimensional. Instead, we obtain a lower bound for δ_{H_Γ} when Γ contains induced subgraphs that satisfy the assumptions of Theorem 4.1.

Definition 5.1 We say that a subgroup H is a *retract* of a group G if there is a homomorphism $r : G \to H$, such that $r : H \to H$ is the identity. We call the homomorphism r a *retraction*.

A standard fact about group retract is that if H is a retract of a finitely presented group G, then H is also finitely presented. The following lemma says that group retractions do not increase Dehn functions.

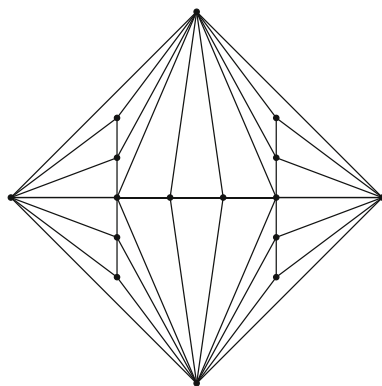**Lemma 5.2** ([7], Lemma 2.2) *If H is a retract of a finitely presented group G, then $\delta_H \preceq \delta_G$.*

Proposition 5.3 *Let Γ be a finite simplicial graph. If Γ' is a connected induced subgraph of Γ, then $H_{\Gamma'}$ is a retract of H_Γ.*

Proof Since Γ' is an induced subgraph of Γ, $A_{\Gamma'}$ is a retract of A_Γ. Let $r : A_\Gamma \to A_{\Gamma'}$ be a retraction; define $r' = r|_{H_\Gamma} : H_\Gamma \to H_{\Gamma'}$. Since Γ and Γ' are connected, H_Γ and $H_{\Gamma'}$ are finitely generated and their generating sets are sets of oriented edges of Γ and Γ', respectively. It suffices to show that r' is the identity on the generating set of $H_{\Gamma'}$. Let e be an oriented edge of Γ' with initial vertex v and terminal vertex w. The generator e of $H_{\Gamma'}$ can be expressed in terms of the generators of $A_{\Gamma'}$, that is, $e = vw^{-1}$. Since $r : A_\Gamma \to A_{\Gamma'}$ is a retraction, we have

$$r'(e) = r(vw^{-1}) = vw^{-1} = e.$$

This shows that $r' : H_\Gamma \to H_{\Gamma'}$ is a retraction. $\qquad\qquad\qquad\square$

We establish the lower bound as promised.

Fig. 43 The graph Γ

Proposition 5.4 *Let Γ be a finite simplicial graph such that Δ_Γ is simply-connected. If Γ contains an induced subgraph Γ' such that $\Delta_{\Gamma'}$ is a 2-dimensional triangulated subdisk of Δ_Γ that has square boundary and $\dim_I(\Delta_{\Gamma'}) = d$, $d \in \{0, 1, 2\}$, then $n^{d+2} \preceq \delta_{H_\Gamma}(n)$.*

Proof By Theorem 4.1, we have $\delta_{H_{\Gamma'}}(n) \simeq n^{d+2}$. Since Γ' is an induced subgraph of Γ, it follows from Proposition 5.3 and Lemma 5.2 that $H_{\Gamma'}$ is a retract of H_Γ and $n^{d+2} \simeq \delta_{H_{\Gamma'}}(n) \preceq \delta_{H_\Gamma}(n)$.   □

We remark that Proposition 5.4 can be used to give the cubic lower bound in Theorem 4.1 for the case $d = 1$. We close this section with an example.

Example 5.5 Let Γ be the graph as shown in Fig. 43:
The flag complex Δ_Γ is not 2-dimensional since Γ contains K_4 subgraphs. Observe that Γ contains an induced subgraph Γ' that is the suspension of a path of length 3. Hence, by Theorem 4.1 and Proposition 5.3, we have $n^3 \simeq \delta_{H_{\Gamma''}}(n) \preceq \delta_{H_\Gamma}(n)$.

References

1. Abrams, A., Brady, N., Dani, P., Duchin, M., Young, R.: Pushing fillings in right-angled Artin groups. J. Lond. Math. Soc. **87**(3), 663–688 (2013)
2. Bestvina, M., Brady, N.: Morse theory and finiteness properties of groups. Invent. Math. **129**(3), 445–470 (1997)
3. Bieri, R.: Normal subgroups in duality groups and in groups of cohomological dimension 2. J. Pure Appl. Algebra **7**(1), 35–51 (1976)
4. Brady, N., Forester, M.: Snowflake geometry in CAT(0) groups. J. Topol. **10**(4), 883–920 (2017)
5. Brady, N., Riley, T., Short, H.: The geometry of the word problem for finitely generated groups. Advanced Courses in Mathematics. CRM Barcelona. Birkhäuser Verlag, Basel, 2007. Papers from the Advanced Course held in Barcelona, July 5–15, (2005)
6. Brady, N., Soroko, I.: Dehn functions of subgroups of right-angled Artin groups. Geom. Dedicata **200**, 197–239 (2019)
7. Brick, S.G.: On Dehn functions and products of groups. Trans. Am. Math. Soc. **335**(1), 369–384 (1993)
8. Bridson, M.R.: The Geometry of the Word Problem. Invitations to Geometry and Topology, Volume 7 of Oxford Graduate Texts in Mathematics, pp. 29–91. Oxford University Press, Oxford (2002)
9. Bridson, M.R., Haefliger, A.: Metric Spaces of Non-positive Curvature. Grundlehren der Mathematischen Wissenschaften (Fundamental Principles of Mathematical Sciences), vol. 319. Springer, Berlin (1999)

10. Carter, W., Forester, M.: The Dehn functions of Stallings–Bieri groups. Math. Ann. **368**(1–2), 671–683 (2017)
11. Charney, R.: An introduction to right-angled Artin groups. Geom. Dedicata **125**, 141–158 (2007)
12. Dicks, W., Leary, I.J.: Presentations for subgroups of Artin groups. Proc. Am. Math. Soc. **127**(2), 343–348 (1999)
13. Dison, W.: An isoperimetric function for Bestvina-Brady groups. Bull. Lond. Math. Soc. **40**(3), 384–394 (2008)
14. Gromov, M.: Hyperbolic Groups. Essays in Group Theory, Volume 8 of Mathematical Science Research Institute Publication, pp. 75–263. Springer, New York (1987)
15. Papadima, S., Suciu, A.: Algebraic invariants for Bestvina-Brady groups. J. Lond. Math. Soc. **76**(2), 273–292 (2007)
16. Stallings, J.: A finitely presented group whose 3-dimensional integral homology is not finitely generated. Am. J. Math. **85**, 541–543 (1963)

Springer